Journal of Assisted Reproduction and Genetics (2022) 39:1901–1908
https://doi.org/10.1007/s10815-022-02566-1

GENETICS

A novel heterozygous variant in PANX1 is associated with oocyte death and female infertility

Xing-Wu Wu[1] · Pei-Pei Liu[1,2] · Yang Zou[2,3] · Ding-Fei Xu[1] · Zhi-Qin Zhang[1] · Li-Yun Cao[1,2] · Lu-Fan[1,2] · Lei-Zhen Xia[1] · Jia-lv Huang[1] · Jia Chen[1] · Cai-Lin Xin[1] · Zhi-Hui Huang[1] · Jun Tan[1,2] · Qiong-Fang Wu[1] · Zeng-Ming Li[2]

Received: 19 February 2022 / Accepted: 4 July 2022 / Published online: 14 July 2022

Abstract

Purpose Oocyte death is a severe clinical phenotype that causes female infertility and recurrent in vitro fertilization and intracytoplasmic sperm injection failure. We aimed to identify pathogenic variants in a female infertility patient with oocyte death phenotype.

Methods Sanger sequencing was performed to screen PANX1 variants in the affected patient. Western blot analysis was used to check the effect of the variant on PANX1 glycosylation pattern in vitro.

Results We identified a novel PANX1 variant (NM_015368.4 c.86G > A, (p. Arg29Gln)) associated with the phenotype of oocyte death in a non-consanguineous family. This variant displayed an autosomal dominant inheritance pattern with reduced penetrance. Western blot analysis confirmed that the missense mutation of PANX1 (c.86G > A) altered the glycosylation pattern in HeLa cells. Moreover, the mutation effects on the function of PANX1 were weaker than recently reported variants.

Conclusion Our findings expand the inheritance pattern of PANX1 variants to an autosomal dominant mode with reduced penetrance and enrich the variational spectrum of PANX1. These results help us to better understand the genetic basis of female infertility with oocyte death.

Keywords PANX1 · Variant · Oocyte death · Female infertility

Introduction

Since the first tube-test baby Luis Brown born in 1978, the assisted reproductive technology (ART), including in vitro fertilization (IVF), and intracytoplasmic sperm injection (ICSI) have helped millions of infertile couples to have a live birth [1]. However, there are still about 30% infertile patients who suffered from recurrent failure of IVF/ICSI attempts [2, 3]. In recent years, several genes, including TUBB8, PATL2, PLCZ1, WEE2, TLE6, PADI6, NLRP2, and NLRP5, have been demonstrated responsible for the defects of oocyte maturation, fertilization, and early embryo development [4–11]. But the genetic factors accounting for the problem are largely unknown.

PANX1 is a highly glycosylated channel protein, which is widely expressed in multiple tissues and organs, especially in brain and oocyte [12]. The main function of PANX1 is release adenosine 5′-triphosphate (ATP) and other small metabolites during intercellular information exchange [13]. In 2019, Qing et al. [12] reported four families with a new phenotype termed oocyte death, which caused recurrent

Xing-Wu Wu, Pei-Pei Liu, and Yang Zou contributed equally to this work.

✉ Jun Tan
tanjun561127@163.com

✉ Qiong-Fang Wu
wuqiongfang898@sina.com

✉ Zeng-Ming Li
lizhengming@163.com

[1] Reproductive Medicine Center, Jiangxi Maternal and Child Health Hospital, Nanchang, Jiangxi 330006, People's Republic of China

[2] JXHC Key Laboratory of Fertility Preservation, Jiangxi Maternal and Child Health Hospital, Nanchang, Jiangxi 330006, People's Republic of China

[3] Central Laboratory, Jiangxi Maternal and Child Health Hospital, Nanchang, Jiangxi 330006, People's Republic of China

IVF/ICSI failure and female infertility, due to heterozygous variants in PANX1 with autosomal dominant (AD) inheritance pattern. In vivo and in vitro experiments demonstrated that these heterozygous mutations led to aberrant PANX1 channel activity and ATP release, and the oocyte death phenotype was recapitulated by overexpression of patients-derived mutation in mice. Recently, Weijie et al. [14] reported novel PANX1 variants in patients with oocyte death phenotype which followed by an autosomal recessive (AR) inherited pattern. This finding demonstrated the critical role of PANX1 in oocyte development. Despite that, the etiology research on oocyte death is far from completeness. Therefore, the mutations and genes involved in oocyte death are still need to be further explored.

In this study, we identified a heterozygous variant in PANX1 (MIM# 608,420) in a non-consanguineous family with the phenotype of oocyte death after fertilization, followed by an autosomal dominant mode with reduced penetrance. This study confirms that PANX1 mutations occur in infertile patients with oocyte death after fertilization, expanding the mutation spectrum of PANX1.

Methods

Human subjects and clinical samples

The infertile patient with the oocyte death phenotype was recruited from Jiangxi Maternal and Child Health Hospital. Peripheral blood samples of the patient and her family members were obtained for DNA extraction. Written informed consent was obtained from the patients. This study was approved by the Ethics Committee of reproductive medicine of the hospital.

Controlled ovarian stimulation

For the first cycle, patient received the gonadotropin-releasing hormone agonist (GnRH-A) protocol. Briefly, standard full dose of GnRH-a (3.75 mg, Ipsen, France) was used in the second day of menstrual cycle for downregulation. Pituitary downregulation (endometrial thickness ≤ 5 mm, serum FSH < 5 mIU/mL, LH < 5 mIU/mL, E2 < 50 pg/mL) was confirmed with transvaginal ultrasound and endocrine examination after 30 days. Then, an initial dose of 150 IU/days of recombinant human FSH (Merck-Serono, German) was used for ovarian stimulation. The time and dose of recombinant human FSH were adjusted according to ovarian response as monitored by serum estradiol levels and vaginal ultrasound. When the dominant follicle was ≥ 19 mm in diameter or at least 2 follicles were ≥ 18 mm in diameter, recombinant human FSH was stopped and a single injection of 250 μg of recombinant hCG (Merck-Serono, German) and 2000 IU urinary-derived hCG (Livzon, China) was administered. Oocyte retrieval was performed 36–40 h later under transvaginal ultrasound guidance. For the second cycle, patient received GnRH antagonist (GnRH-ant) protocol. Ovarian stimulation was started with 200 IU of recombinant human FSH (rhFSH, Merck-Serono, German) treatment on day 2 of the menstrual cycle. The daily dose of rhFSH was adjusted according to ovarian response as monitored by ultrasonography and serum estradiol (E_2) levels. GnRH antagonist (Cetrorelix, Merck Serono, Switzerland) at a daily dose of 0.25 mg was started when the largest follicle exceeded 12 mm. Both GnRH antagonist and rhFSH were stopped and a single injection of 250 ug of recombinant hCG (Merck-Serono, German), and 2000 IU urinary-derived hCG (Livzon, China) was administered when the dominant follicle was ≥ 19 mm in diameter or at least 2 follicles were ≥ 18 mm in diameter. Oocyte retrieval was performed 36–40 h later under transvaginal ultrasound guidance.

Evaluation of oocyte and embryo phenotypes

Oocytes were obtained from patient and controls undergoing clinical IVF/ICSI. The morphologies of oocytes, fertilization, and embryonic development were evaluated by light microscopy. The assessment was made in a blinded manner by two embryologists.

Screening of PANX1 variants

Genomic DNA samples of the proband and her family members were extracted from peripheral blood using the QIAamp DNA Blood Mini Kit (Qiagen, Germany). The DNA concentration and purity were measured with a NanoDrop 1000 spectrophotometer (Thermo Scientific, USA). All exons of PANX1 were amplified, and the corresponding primers are shown in Table 1. Then, Sanger sequencing was performed to identify mutation in PANX1. Amplified fragments were directly sequenced using an ABI 3100 DNA analyzer (Applied Biosystems, USA). The novel PANX1 variant was submitted to Leiden Open Variation Database (LOVD) at https://www.LOVD.nl/PANX1.

Expression vector construction

The full length of PANX1 encoding sequence was amplified and cloned into the pcDNA3.1 vector. Site-directed mutagenesis was performed to introduce the identified variant c.86G > A (p. Arg29Gln) into the wild-type (WT) vector. And the WT and mutant clones were confirmed by Sanger sequencing.

Table 1 Primers used for PANX1 exon amplification and sequencing

Primer name	Primer sequence
PANX1-Exon1-F1	TGAGGCACCGAGACACAAG
PANX1-Exon1-R1	CGTAAAATCGCAGCTCACCG
PANX1-Exon1-F2	AGGCACCGAGACACAAAGG
PANX1-Exon1-R2	GCTCACGACCATCACAGCT
PANX1-Exon2-F	TCTCCACCTCCTGTCCTGG
PANX1-Exon2-R	AACACTTCCCATTGCCCCA
PANX1-Exon3-F	ATCACTTGGCGCCATAGGTT
PANX1-Exon3-R	GGCTGTCACTAGGTGCATGA
PANX1-Exon4-F	TTTGACTACTGACGTTGTAGGT
PANX1-Exon4-R	CCTACCCCGCACCTTGGTA
PANX1-Exon5-F1	GGCCAAGAAGCAAAACATGGT
PANX1-Exon5-R1	TGAAACCAACAGGGGTGCTT
PANX1-Exon5-F2	ACCTCTGATCTCCTTCTCTGT
PANX1-Exon5-R2	TCCCATGTCGCAGAAGTCAC

Cell culture and transfection

HeLa cells obtained from the cell bank of Shanghai Institute for biological sciences were cultured in high-glucose Dulbecco's minimum essential medium (Gibco, USA) supplemented with 1% penicillin/streptomycin and 10% of (v/v) fetal bovine serum (FBS; Gibco, USA) and cultured in a humidified 5% CO_2 incubator at 37 ℃. PANX1 WT, mutant construct, and the pcDNA3.1 vector were transfected into HeLa cells using the FuGENE HD Transfection Reagent (Promega, USA) according to the manufacturer's instructions.

Western blotting

HeLa cells were harvested 36 h after transfection and washed three times with cold phosphate-buffered saline (PBS). Cells were lysed in RIPA lysis buffer with 1% of protease inhibitor cocktail (Applygen, China) and centrifuged at 12,000 × g for 30 min at 4 ℃. Supernatants were collected, mixed with 5 × sodium dodecyl sulfate (SDS) loading buffer, and heated at 100 ℃ for 10 min. Equal amounts of protein were separated using SDS–polyacrylamide gel electrophoresis and transferred to PVDF membranes (Merk-Milipore, USA). The membranes were blocked with 5% nonfat milk diluted in PBS with 0.1% of Tween 20 (PBST) for 1 h and then incubated at 4 ℃ overnight with rabbit anti-PANX1 (1:1000 dilution, Cell Signaling Technology, USA) and rabbit anti-GAPDH (1:1000 dilution, Cell Signaling Technology, USA). The membranes were washed with PBST three times and incubated with goat anti-rabbit IgG secondary antibodies (1:5000 dilution, Immunoway, USA) for 1 h at room temperature followed by washing again with PBST three times. Finally, the membranes were incubated with ECL western blotting Substrate (Tanon, China) and imaged on a chemiluminescent imaging system (5200, Tanon, China). Quantitation of western blotting results was performed with the ImageJ software.

Statistical analyses

All data are representative of at three independent experiments. SPSS 24.0 software was used to perform the statistical analysis. Values were analyzed by Student's *t* tests when comparing experimental groups, and P values < 0.05 were considered statistically significant.

Result

Clinical characteristics of the proband

The proband from a non-consanguineous family had been diagnosed with primary infertility for several years. She was 33 years old at examination and had normal menstrual cycles and normal sex hormone level. The seminal parameters of her husband showed 60 million per milliliter of sperm concentration, 35% progressive motility, and 9.5% normal sperm morphology per ejaculate. She had undergone a failed IVF and a failed ICSI treatment cycle. In the IVF attempt, an early follicular phase agonist long protocol was conducted for controlled ovarian stimulation. The estradiol level on day of hCG trigger was 2126 pg/ml. A total of 10 oocytes were retrieved, and all of them were successfully fertilized. However, all fertilized oocyte were gradually degenerated and died within 40 h, characterized by shrinking and blackening of the oocyte cytoplasm. In the ICSI attempt, the ovarian stimulation protocol was changed to antagonist protocol. The estradiol level on day of hCG trigger was 1223 pg/ml. Eleven oocytes were retrieved, and 7 out of 8 metaphase II oocytes were successfully fertilized by ICSI. However, all fertilized oocytes were degenerated and died within 40 h and 2 of them died after finished the first cleavage (Table 2; Fig. 1).

Identification of heterozygous variants in PANX1

Previous study had shown that PANX1 mutations can lead to oocyte death phenotype. Due to the clinical characteristics and oocyte death phenotype of the proband, screening of PANX1 variants was performed. Most of members in the family underwent Sanger sequencing of PANX1 exons. As we expected, the proband carries a heterozygous mutation c.86G > A (p. Arg29Gln)) in PANX1, which is inherited from her father (Figs. 2 and 3). And her aunt (II-3) and cousin (III-6) were also the heterozygous missense mutation carrier. However, the proband's aunt (II-3) carry this variant, which had given birth to a son 17 years ago by herself

Table 2 Clinical characteristics of IVF attempts of the proband

IVF attempts	Insemination method	Total oocytes	MII oocytes	Fertilized oocytes	Oocytes died after fertilization	Zygotes died after the first cleavage	Usable embryos
No. 1	IVF	10	10	10	10	0	0
No. 2	ICSI	11	8	7	5	2	0

IVF in vitro fertilization, *ICSI* intracytoplasmic sperm injection

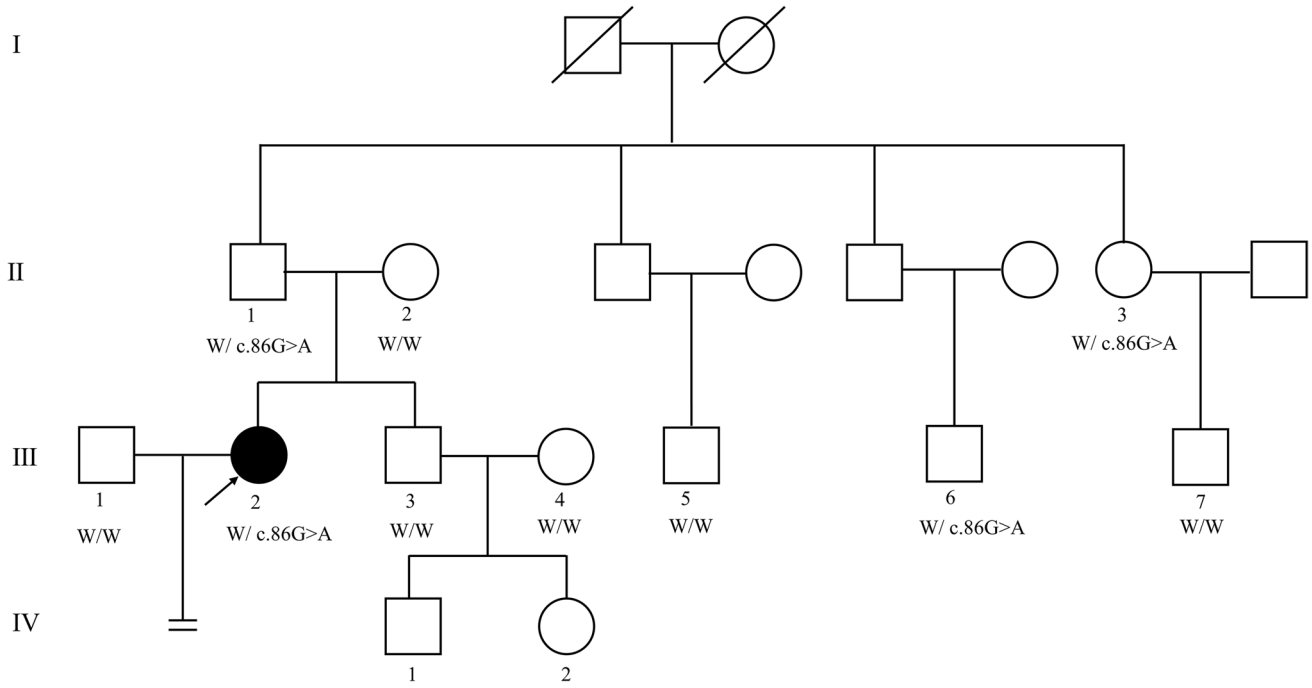

Fig. 1 Morphology of oocytes retrieved from control individuals and proband at 0 h, 20 h, 28 h, and 40 h. All fertilized oocytes were died within 40 h, and 2 of them died after the first cleavage. Scale bar, 40 μm

without ART treatment or egg donation program (Figs. 2 and 3). This suggests that this variant displays a distinguished expressivity in different contexts.

Function prediction of the PANX1 mutation

The mutation in the family was absent in the population according to 1000 Genomes Browser (http://www.internationalgenome.org/) or Genome Aggregation Database (https://gnomad.broadinstitute.org/). The location of mutation in PANX1 and PANX1 protein is shown in Table 3 and Fig. 4 A and B. Variation c.86G > A was located in exon 1 and caused an amino acid substitution a position 29 in N-terminal loop of PANX1 protein. The residue Arg29 was highly conserved across species (Fig. 4C). The pathogenicity of the variant was assessed using three online software: mutation taster (www.mutationtaster.org/), SIFT (sift.jcvi.org), and PloyPhen2 (genetics.bwh.harvard.edu/pph2/). As shown in Table 2, the missense mutation c.86G > A (p. Arg29Gln)) of PANX1 was predicted to be pathogenic by mutation taster, SIFT, and PloyPhen2.

Effect of heterozygous variant on PANX1 glycosylation in vitro

PANX1 exists in three glycosylation states: the non-glycosylation protein (GLY0), a high-mannose glycoprotein (GLY1), and a fully mature glycoprotein (GLY2). To investigate the effects of the mutation we identified on PANX1 glycosylation in vitro, we examined the HeLa cells 36 h after transfection with WT or mutant construct. Compared with WT PANX1, the (p. Arg29Gln) variant resulted in a significantly reduced the GLY2 species and the GLY2/GLY1 intensity ratio (Fig. 4D and F), which is consist with the p. (Arg300Gln) and p. (Cys347Ser) [14]. These results indicated that the PANX1 variant (p. Arg29Gln) resulted in an altered glycosylation pattern in HeLa cell in vitro.

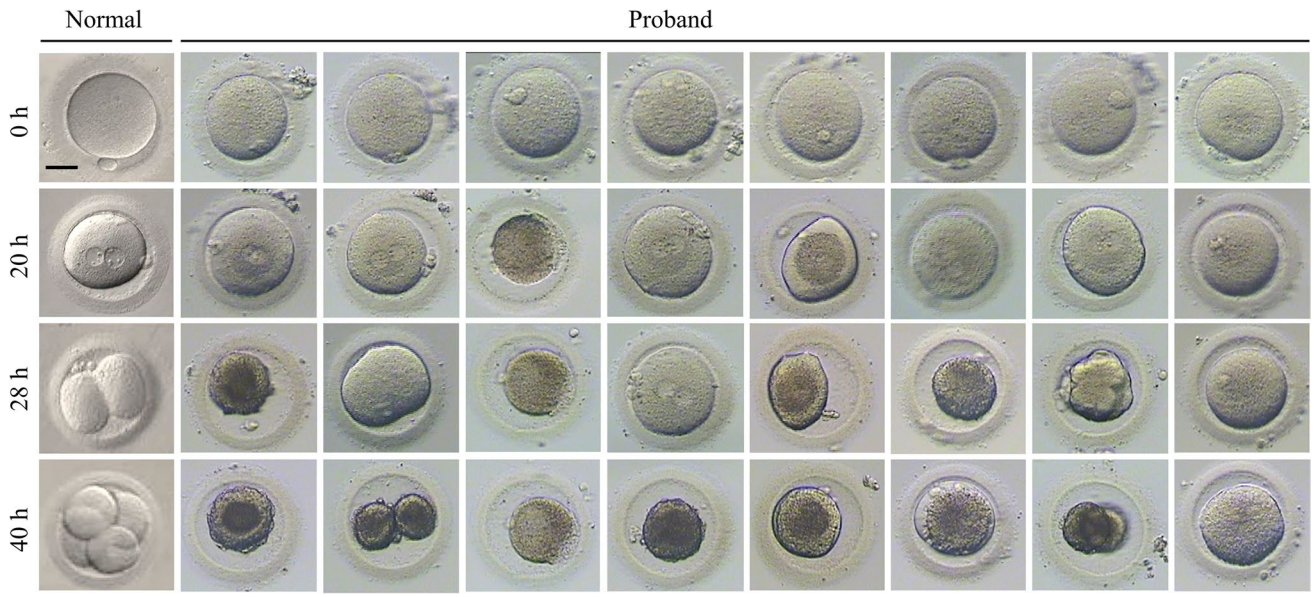

Fig. 2 A pedigree with PANX1 mutation cause infertility with oocyte death phenotype. Squares indicate male family member, circles indicate female members, black solid circle with arrow indicates the proband, the equal sign indicates infertility, and "W" indicates wild-type allele

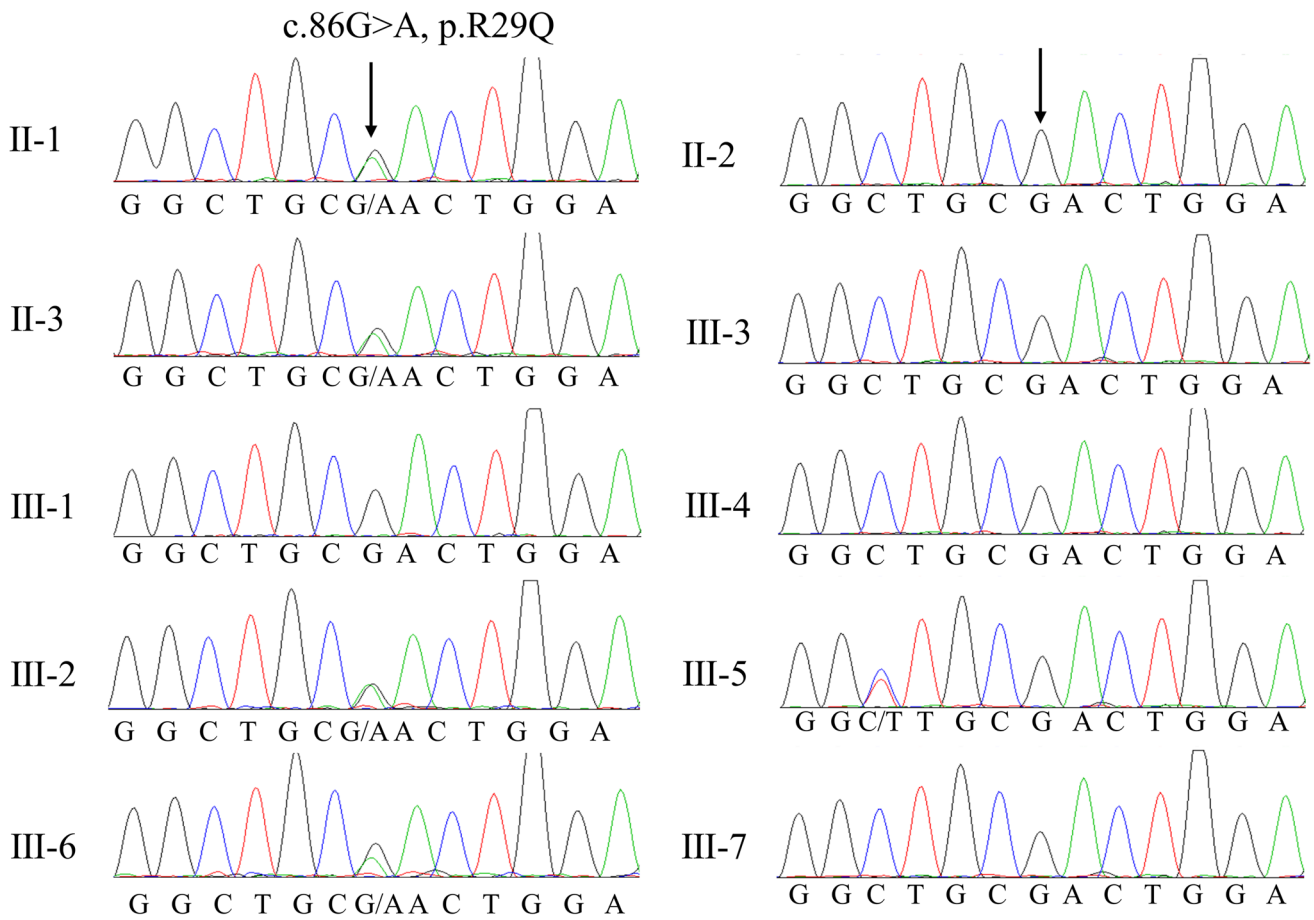

Fig. 3 Sanger sequencing results of the proband and her family members

Table 3 Overview of the PANX1 mutation

Genomic position on Chr11	cDNA change	Protein change	Variant type	Inheritance	GnomAD†	1000 genomes†	SIFT*	PloyPhen2*	Mutation taster*
93,862,564	c.G86 > A	p. Arg29Gln	Missense	AD	Not found	Not found	Damaging	Probably damaging	Deleterious

AD autosomal dominant

†Frequency of corresponding mutation in GnomAD and 1000 Genomes Browser

*Mutation assessment by SIFT, PloyPhen2 and Mutation taster

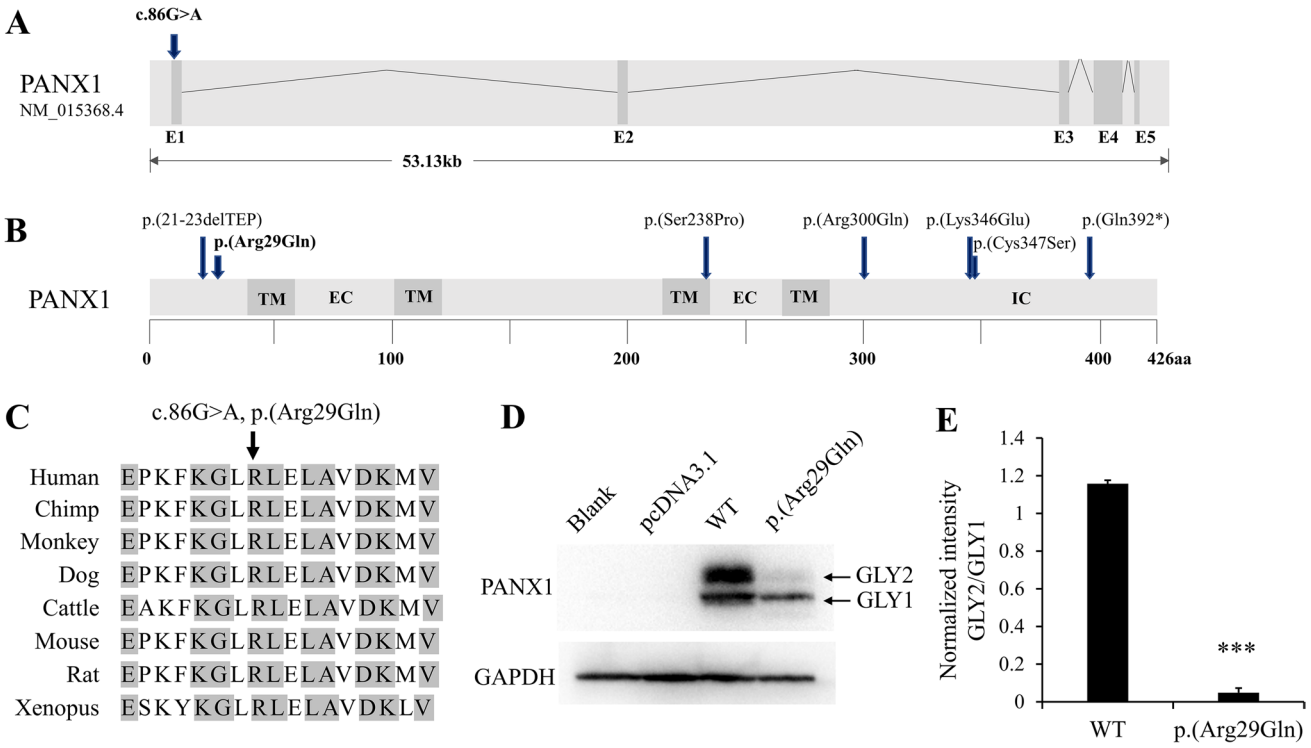

Fig. 4 Mutation location of PANX1 variant and conservation analysis of the affected amino acid. **A** Location of the newly identified heterozygous variant in PANX1 exon. **B** Location of mutations in the PANX1 protein; the bold font indicates the newly identified variant and the thin font indicate the variants discovered previously [11, 13]. TM, transmembrane region; EC, extracellular region; IC, intracellular region. **C** Conservation analysis of the affected amino acid among eight species. **D** Western blot analysis of HeLa cell extracts after transfection with WT or mutant PANX1 constructs. GAPDH was used as the loading control. **E** The ratio of GLY2 to GLY1 of PANX1. The GLY1/GLY1 of (p. Arg29Gln) variant was significantly reduced compared with WT. Three independent experiments were performed; ***$P < 0.001$

Discussion

In this study, we identified a heterozygous variant (c.86G > A (p. Arg29Gln)) in PANX1 from a non-consanguineous family with the phenotype of oocyte death after fertilization. Unlike the previously reported inheritance pattern, the variant showed an autosomal dominant inheritance pattern with reduced penetrance. And we confirmed that the heterozygous variant altered the PANX1 glycosylation pattern in cultured cells.

Qing et al. [12] firstly reported four heterozygous variants (c.1174C > T (p. (Gln392*)), c.1036A > G (p. (Lys346Glu)), c.1040G > C (p. (Cys347Ser)), and c.61_69delACGGAG CCC (p.(21_23delTEP))) in PANX1 are responsible for oocyte death in 2019. They demonstrated that the mutations altered the PANX1 glycosylation pattern and led to

aberrant PANX1 channel activity and ATP release in oocytes by in vitro and in vivo experiments. In the present study, heterozygous variant c.86G > A (p. Arg29Gln) in PANX1 was shown to cause oocyte death and followed by an irregular AD inheritance pattern. More recently, Weijie et al. [14] reported two homozygous variants c.712 T > C (p. (Ser238Pro)) and c.899G > A (p. (Arg300Gln)) in PANX1, which were also shown to cause oocyte death with an AR pattern. These findings suggested that mutations in different locations in PANX1 might appear different effects on the protein and the inheritance patterns might arise by different effects of the mutations accordingly.

Previous reported that heterozygous variants c.1174C > T (p. (Gln392*)) and c.1036A > G (p. (Lys346Glu)) had a more severe phenotype with oocyte death before fertilization, while the heterozygous variants c.1040G > C (p. (Cys347Ser)) and c.61_69delACGGAGCCC (p.(21_23delTEP)) did not die until after fertilization [12]. In this study, the proband with heterozygous mutation c.86G > A (p. Arg29Gln)) had the phenotype of oocyte death after fertilization or the first cleavage. These results suggested that mutation's location affected the phenotype severity. Several studies on the structure of PANX1 have shown that it was a heptameric channel protein and played an important role in cellular communication [15–20]. Moreover, the C-terminal domain and the N-terminal loop which extended toward the intracellular region might serve as a channel gate for ion permeation or ion selectivity [18, 20]. This may explain why the heterozygous mutations p. (Gln392*) and p. (Lys346Glu) which located in the C-terminal domain had a more severe phenotype than heterozygous variants p. (Cys347Ser), p.(21_23delTEP) and (p. Arg29Gln) (Fig. 4B). And the variants p. (Ser238Pro) and p. (Arg300Gln), which located near the transmembrane regions, resulted in oocyte death only in a homozygous state (Fig. 4B).

There is also a phenotype difference between women with heterozygous variants. The proband with the variant c. 86G > A had all oocyte death after fertilization (2 of them died while finished the first cleavage) (Fig. 1), while her aunt (II-3) has given a live birth of a son 17 years ago (Fig. 2). Additionally, as Weijie et al. [14] reported that patients with homozygous variant c.899G > A (p. (Arg300Gln)) could produce a viable embryo during IVF treatment. PANX1 is a glycoprotein that exists in different glycosylated forms and the glycosylation level is critical for cellular localization and function [21]. It is likely that the phenotype severity of PANX1 variant depends on the impairment of glycosylation functioned by modifying genes.

Previous studies have found that panx1 knockout mice were fertile and have no obvious reproductive defects [22]. And the engineered OE-PANX1^{Q392*} female mice were completely infertile with the oocyte death phenotype [12], implying that the oocyte death phenotype was caused by a gain-of-function effect. The newly identified heterozygous variant c.86G > A (Fig. 3) and two previously reported heterozygous variants c.1040G > C and c.61_69delACGGAGCCC [12] in PANX1 resulted in oocyte death only after fertilization, but the molecular mechanism for this phenotype remains unknown. During fertilization, oocyte activation consists of a coordinated series of events [23], including repeated increases in cytoplasmic calcium concentration, cortical granule exocytosis, the resumption of the second phase of meiosis, and extrusion of the second polar body. We speculated that oocyte death after fertilization might be related to these intense ions exchanged and highly ATP consumption processes, and this requires further exploration in transgenic mice.

Conclusion

In brief, we have identified the heterozygous variant c.86G > A (p. Arg29Gln)) in PANX1 as responsible for oocyte death and female infertility. Our finding expands the spectrum of PANX1 mutation and provides genetic evidence for infertile women with oocyte death during IVF treatment.

Acknowledgements We sincerely thank the patient and her family for their participation and support in this study.

Author contribution JT, QW, and ZL conceived and designed the study. DX, ZZ, CX, and ZH contributed to the recruitment, characterization, and oocyte image of the patient. PL, LC, and LF performed the exon sequencing. PL performed the cell culture, expression vector transfection, and western blot. And LX and JH organized the medical records. XW, JC, and YZ contributed to the bioinformatics analysis. XW and JT wrote the draft of the manuscript. All the authors commented on previous version of the manuscript and approved the final manuscript.

Funding This work was supported by the National Natural Science Foundation of China (81960271 and 81960288), the Major Research and Development Project of Science and Technology Department of Jiangxi Province (20203BBGL73140), and the JXHC Key Laboratory of Fertility Preservation.

Data availability All data generated and analyzed in this study are included in this published manuscript.

Declarations

Ethics approval and consent to participate This study was conducted in accordance with the guidelines of the Declaration of Helsinki and was approved by the Clinical Ethical Committee of Jiangxi Maternal and Child Health Hospital, and informed consents from patient were obtained before the initiation of the study. All the authors consented to participate in this study.

Consent for publication All the authors consented for publication.

Conflict of interest The authors declare no competing interests.

References

1. Boseley S. IVF at 40. The Lancet. 2018;392(10145):376–7. https://doi.org/10.1016/s0140-6736(18)31662-3.
2. Malizia BA, Hacker MR, Penzias AS. Cumulative live-birth rates after in vitro fertilization. N Engl J Med. 2009;360(3):236–43. https://doi.org/10.1056/NEJMoa0803072.
3. Smith A, Tilling K, Nelson SM, et al. Live-birth rate associated with repeat in vitro fertilization treatment cycles. JAMA. 2015;314(24):2654–62. https://doi.org/10.1001/jama.2015.17296.
4. Alazami AM, Awad SM, Coskun S, et al. TLE6 mutation causes the earliest known human embryonic lethality. Genome Biol. 2015;16:240. https://doi.org/10.1186/s13059-015-0792-0.
5. Chen B, Zhang Z, Sun X, et al. Biallelic mutations in PATL2 cause female infertility characterized by oocyte maturation arrest. Am J Hum Genet. 2017;101(4):609–15. https://doi.org/10.1016/j.ajhg.2017.08.018.
6. Feng R, Sang Q, Kuang Y, et al. Mutations in TUBB8 and human oocyte meiotic arrest. N Engl J Med. 2016;374(3):223–32. https://doi.org/10.1056/NEJMoa1510791.
7. Mu J, Wang W, Chen B, et al. Mutations in NLRP2 and NLRP5 cause female infertility characterised by early embryonic arrest. J Med Genet. 2019;56(7):471–80. https://doi.org/10.1136/jmedgenet-2018-105936.
8. Sang Q, Li B, Kuang Y, et al. Homozygous mutations in WEE2 cause fertilization failure and female infertility. Am J Hum Genet. 2018;102(4):649–57. https://doi.org/10.1016/j.ajhg.2018.02.015.
9. Sang Q, Zhou Z, Mu J, et al. Genetic factors as potential molecular markers of human oocyte and embryo quality. J Assist Reprod Genet. 2021;38(5):993–1002. https://doi.org/10.1007/s10815-021-02196-z.
10. Xu Y, Shi Y, Fu J, et al. Mutations in PADI6 cause female infertility characterized by early embryonic arrest. Am J Hum Genet. 2016;99(3):744–52. https://doi.org/10.1016/j.ajhg.2016.06.024.
11. Kashir J, Konstantinidis M, Jones C, et al. A maternally inherited autosomal point mutation in human phospholipase C zeta (PLC-zeta) leads to male infertility. Hum Reprod. 2012;27(1):222–31. https://doi.org/10.1093/humrep/der384.
12. Sang Q, Zhang Z, Shi J et al. A pannexin 1 channelopathy causes human oocyte death. Sci Transl Med 2019, 11(485). https://doi.org/10.1126/scitranslmed.aav8731
13. Bao L, Locovei S, Dahl G. Pannexin membrane channels are mechanosensitive conduits for ATP. FEBS Lett. 2004;572(1–3):65–8. https://doi.org/10.1016/j.febslet.2004.07.009.
14. Wang W, Qu R, Dou Q, et al. Homozygous variants in PANX1 cause human oocyte death and female infertility. Eur J Hum Genet. 2021. https://doi.org/10.1038/s41431-020-00807-4.
15. Deng Z, He Z, Maksaev G, et al. Cryo-EM structures of the ATP release channel pannexin 1. Nat Struct Mol Biol. 2020;27(4):373–81. https://doi.org/10.1038/s41594-020-0401-0.
16. Michalski K, Syrjanen JL, Henze E et al. The Cryo-EM structure of pannexin 1 reveals unique motifs for ion selection and inhibition. Elife 2020, 9. https://doi.org/10.7554/eLife.54670
17. Qu R, Dong L, Zhang J, et al. Cryo-EM structure of human heptameric pannexin 1 channel. Cell Res. 2020;30(5):446–8. https://doi.org/10.1038/s41422-020-0298-5.
18. Mou L, Ke M, Song M, et al. Structural basis for gating mechanism of pannexin 1 channel. Cell Res. 2020;30(5):452–4. https://doi.org/10.1038/s41422-020-0313-x.
19. Jin Q, Zhang B, Zheng X, et al. Cryo-EM structures of human pannexin 1 channel. Cell Res. 2020;30(5):449–51. https://doi.org/10.1038/s41422-020-0310-0.
20. Ruan Z, Orozco IJ, Du J, et al. Structures of human pannexin 1 reveal ion pathways and mechanism of gating. Nature. 2020;584(7822):646–51. https://doi.org/10.1038/s41586-020-2357-y.
21. Penuela S, Simek J, Thompson RJ. Regulation of pannexin channels by post-translational modifications. FEBS Lett. 2014;588(8):1411–5. https://doi.org/10.1016/j.febslet.2014.01.028.
22. Zhao HB, Zhu Y, Liang C, et al. Pannexin 1 deficiency can induce hearing loss. Biochem Biophys Res Commun. 2015;463(1–2):143–7. https://doi.org/10.1016/j.bbrc.2015.05.049.
23. Tosti E, Menezo Y. Gamete activation: basic knowledge and clinical applications. Hum Reprod Update. 2016;22(4):420–39. https://doi.org/10.1093/humupd/dmw014.